ARDS neutrophils have a distinct phenotype and are resistant to phosphoinositide 3-kinase inhibition

Juss JK[1#], House D[2], Amour A[2], Begg M[2], Herre J[3], Storisteanu DML[1], Hoenderdos K[1], Bradley G[4], Lennon M[4], Summers C[1], Hessel EM[2], Condliffe AM[1*] Chilvers ER[1*]

[1]Department of Medicine, University of Cambridge UK, [2]Refractory Respiratory Inflammation Discovery Performance Unit, GlaxoSmithKline, Stevenage, UK, [3]Cambridge University Hospitals NHS Foundation Trust and [4]Target Sciences, GlaxoSmithKline, Stevenage, UK

* These authors made an equal contribution
# Current address: Li Ka Shing Knowledge Institute, St. Michael's Hospital, Toronto, Canada

Author contributions: JKJ, ERC, AMC, DH, AA, MB, CS and EMH contributed to the concept and/or design of the study.   JKJ, AA, DMLS and KH contributed to the acquisition of the data, and all authors contributed to the analysis and interpretation. JKJ, AMC and

ERC drafted the manuscript, and all authors critically revised it for intellectual content and approved the final version prior to submission.

Correspondence: Professor Edwin R Chilvers PhD, FRCP, FMedSci, ScD. Department of Medicine, University of Cambridge School of Clinical Medicine, Box 157 Addenbrooke's Hospital, Hills Road, Cambridge CB2 0QQ, UK. erc24@cam.ac.uk, (+44) 1223 762007

Running title: Phenotype of ARDS alveolar and blood neutrophils

ABSTRACT

Rationale: The acute respiratory distress syndrome is refractory to pharmacological intervention. Inappropriate activation of alveolar neutrophils is believed to underpin this disease's complex pathophysiology, yet these cells have been little studied.

Objectives: To examine the functional and transcriptional profiles of patient blood and alveolar neutrophils compared to healthy volunteer cells, and define their sensitivity to phosphoinositide 3-kinase inhibition.

Methods: Twenty three ventilated patients underwent bronchoalveolar lavage. Alveolar and blood neutrophil apoptosis, phagocytosis and adhesion molecules were quantified by flow cytometry, and oxidase responses by chemiluminescence. Cytokine and transcriptional profiling utilized multiplex and GeneChip arrays.

Measurements and Main Results: Patient blood and alveolar neutrophils were distinct from healthy circulating cells, with increased CD11b and reduced CD62L expression, delayed constitutive apoptosis and primed oxidase responses. Incubating control cells with disease bronchoalveolar lavage recapitulated the aberrant functional phenotype and this could be reversed by phosphoinositide 3-kinase inhibitors. In contrast, the pro-survival phenotype of patient cells was resistant to phosphoinositide 3-kinase inhibition. RNA transcriptomic analysis revealed modified immune, cytoskeletal and cell death pathways in patient cells, aligning closely to sepsis and burns data sets but not phosphoinositide 3-kinase signatures.

Conclusions: Acute respiratory distress syndrome blood and alveolar neutrophils display a distinct primed, pro-survival profile and transcriptional signature. The enhanced respiratory burst was phosphoinositide 3-kinase-dependent, but delayed apoptosis and the altered transcriptional profile were not. These unexpected findings cast doubt over the utility of phosphoinositide 3-kinase inhibition in acute respiratory distress syndrome and highlight the importance of evaluating novel therapeutic strategies in patient-derived cells.

INTRODUCTION

The acute respiratory distress syndrome (ARDS) is characterised by diffuse alveolar injury and immune cell infiltration, resulting in intractable hypoxemia [1]. Despite the adoption of lung-protective ventilation, mortality remains high [2], and many survivors suffer long-term physical or neurocognitive sequelae, with fewer than 50% returning to work [2]. Management remains largely supportive with optimisation of ventilator parameters [3], judicious fluid balance, and treatment of underlying causes; no pharmacological interventions have proven beneficial.

Accumulation of neutrophils (PMNs) in the lung microvasculature, interstitial and alveolar compartments is a key feature of ARDS [4], and association has been reported between intensity of alveolar neutrophil infiltration and disease severity [5]. Inappropriate accumulation/activation of PMNs within the alveoli is proposed to cause unrestrained release of oxygen radicals, proteases and neutrophil extracellular traps (NETs). Due to challenges inherent in isolating alveolar PMNs (alvPMNs), their functional activity in ARDS is largely unknown. Historically, mouse models have been used as surrogates for alvPMNs [6]; however, rodent neutrophils differ markedly from their human counterparts.

Traditionally PMNs have been viewed as a homogenous population of short-lived cells with limited transcriptional capacity and a fixed functional repertoire. More recently, concepts of long-lived PMNs, retrograde trans-endothelial migration and PMN plasticity have emerged [7-12]. Given recent demonstrations that PMNs can modify their transcriptional profile following an inflammatory insult [13], genome-wide transcriptional analysis provides a powerful tool to identify novel targets relevant to altered PMN functions, and has been

successfully applied in asthma, pulmonary arterial hypertension and ARDS [14]; however, studies in ARDS are based on the analysis of total peripheral white blood cells rather than purified neutrophils.

Lung epithelial cells [15] synthesize granulocyte macrophage-colony stimulating factor (GM-CSF), a cytokine essential for alveolar macrophage function [16-17] and surfactant homeostasis [18-19]. Conversely, during inflammation GM-CSF potentiates superoxide-anion production [20], promotes PMN survival [21], and is detrimental in models of acute lung injury [22]. PMN longevity increases dramatically in ARDS, and some studies have identified GM-CSF as a major pro-survival mediator [23]. Whilst the molecular mechanisms governing PMN lifespan in ARDS are incompletely understood, the cytoprotective effect of GM-CSF in PMNs *in vitro* is Class 1 phosphoinositide 3-kinase (PI3K)-dependent [21]. PI3K inhibition prevents lung tissue edema and leukocyte recruitment in models of ARDS [24], and inhibition of PI3Kγ in a sepsis model reduces end-organ damage [25]. Following the early exuberant pro-inflammatory response in ARDS, patients develop immune-paresis, increasing susceptibility to nosocomial infections [26]; recent studies demonstrate that inhibition of PI3Kδ may improve PMN responses during this phase [27]. These observations have triggered considerable interest in the therapeutic use of PI3K inhibitors in ARDS.

Herein we present the first comprehensive characterization of purified ARDS blood ([blood]PMN) and [alv]PMNs and the first genome-wide transcriptome analysis of purified ARDS [blood]PMNs. We show that ARDS [alv]PMNs are hyper-segmented, with enhanced CD11b and reduced CD62L expression, and display delayed apoptosis but preserved oxidative burst, phagocytosis and neutrophil extracellular trap (NET) responses. ARDS [blood]PMNs display an intermediate phenotype, with a transcriptome showing significant alterations in cell-survival

and inflammatory pathways, but little overlap with the PI3K-dependent gene signature. This work improves our understanding of PMN function in ARDS and reveals that apoptosis of ARDS neutrophils is resistant to PI3K inhibition. Together, these observations strengthen the case to modulate PMN function in ARDS, but cast doubt over the utility of PI3K inhibitors in this condition. Some results from these studies have been reported in the form of an abstract [28].

MATERIALS and METHODS

Ethics

All studies complied with the Declaration of Helsinki. Written informed consent was obtained from the legal surrogate of ARDS patients (UK08/H0306/17). Paired blood samples were obtained simultaneously from age and gender matched healthy volunteers (HV) (UK06/Q0108/281).

Bronchoalveolar lavage

Patients fulfilling the Berlin criteria for ARDS [29] were recruited from mixed medical/surgical and neurosciences/trauma intensive care units in a UK teaching hospital; exclusion criteria were age <18 years, HIV positive, or if informed assent could not be obtained. The median tidal volume in the ARDS patients was 7.64 ml per kilogram Predicted Body Weight (IQR=6.94-8.64 ml/kg). Patients underwent venepuncture, bronchoscopy (FOB) and bronchoalveolar lavage (BAL) within 48 hours of diagnosis. Sterile isotonic saline (3x50 ml) was instilled into a sub-segmental bronchus; recovery averaged 90 ml (range 20-120 ml) and did not differ between patients and controls. BALF was immediately filtered and placed on ice. Control BALF was collected from patients (n=10) undergoing elective FOB for indications unrelated to infection or ARDS.

PMN purification

[alv]PMN and autologous [blood]PMN were isolated from patients alongside [blood]PMN from age and gender-matched HVs. Alveolar PMNs were purified by immune-magnetic negative selection (RoboSep⁻, StemCell Technologies) [30] to >90% purity and >98% viability. [blood]PMNs were purified over discontinuous plasma-Percoll gradients [28].

PMN morphology

PMN were classified by nuclear morphology, with the assessor blinded to sample origin. Mature PMN displayed 3-4 nuclear lobes connected by heterochromatin filaments. Band PMNs had less condensed chromatin and incompletely segmented nuclei [31], whilst hyper-segmented PMNs possessed ≥5 lobes.

PMN activation and apoptosis

HV and ARDS [blood]PMNs and unprocessed BALF were re-suspended in PBS containing 5% BSA and protease inhibitor cocktail (Complete Mini EDTA-free, Roche). Samples were stained with CD62L-APC (BD Pharmingen-clone 559772), CD11b-FITC (Beckman Coulter clone IM0530) or isotype-matched controls. PMN apoptosis was assessed after 20 hours by flow cytometry using FITC-labelled Annexin-V/propidium iodide (AnV/PI, BD-Pharmingen).

PMN oxidative burst

Neutrophils (5×10^6/mL) were primed with tumor necrosis factor (TNF)-α (R&D Systems), GM-CSF, control BALF or ARDS BALF at 37°C for 30 minutes. The oxidative burst in

response to fMLP (100 nM), zymosan or heat-killed *Streptococcus pneumoniae* (serum-opsonized, 5-7 particles/PMN) was assessed by luminol-dependent chemiluminescence [30].

Quantification of inflammatory mediators

BALF and serum mediators were measured by ELISA (LPS (Kamiya), survivin and LTB_4 (R&D Systems)), or using the Human Biomarker 40-Plex V-PLEX Kit and Human MMP 3-Plex Ultra-Sensitive Kit (MesoScale Discovery). Where stated BALF samples were corrected to the total protein concentration (Pierce™ BCA-Protein Assay).

PMN phagocytosis

PMN phagocytic capacity was assessed using 1 mg/ml pHrodo™ RED *Staphylococcus aureus* Bioparticles® (Life Technologies). Internalization was verified by live confocal imaging.

NET formation

[blood]PMNs and [alv]PMNs (1×10^6/ml) incubated with Sytox Green (5 μM, Life Technologies) were seeded onto 96 well optical microplates (BD Biosciences). NET formation was quantitated by hourly fluorescence measurements and verified by fluorescence microscopy using rabbit anti-histone H3 (Ab5103, Abcam).

Neutrophil cytoskeletal remodelling

Freshly isolated PMNs (1×10^6/ml) were fixed (4% PFA), permeabilized (0.5% Triton) and stained with anti-neutrophil elastase (Santa Cruz, 1:1,000) and rhodamine phalloidin 1:200 (Invitrogen).

Genome-wide transcriptomic changes

Genome-wide transcriptomic changes were assessed in paired blood PMNs from n=12 consecutively recruited ARDS patients, who were representative of the full patient cohort in terms of age, gender, ARDS severity and causation, and n=12 HVs. Further studies were undertaken in the following groups of HV [blood]PMNs (n=10/group): (a) T=0 hours vehicle control, (b) T=6 hours vehicle control, (c) T=6 hours rhGM-CSF (1 ng/ml), (d) T=6 hours panPI3K inhibitor ZSTK474 (10 μM), and (e) T=6 hours rhGM-CSF plus ZSTK474.

cDNA prepared from 2.5 ng RNA using WT-Ovation Pico RNA Amplification System (NuGen) was fragmented and labelled using FL-Ovation cDNA Biotin Module V2 (NuGen). Labelled cDNA was hybridized onto Hg-U133 Plus 2.0 GeneChip oligonucleotide arrays (Affymetrix). Raw data (see 'Additional Materials' supplement') were normalised using the Robust Multi-array Average (RMA) method [32] and Quality Checked in R/Bioconductor. A linear model was fitted to normalised data for each probe set and a post-hoc test (Fisher LSD) generated fold changes and p-values. Probes were identified as significant if their fold change was >1.5 and $p<0.05$, and mapped to pathways using Ingenuity Pathway Analysis software. The NextBio analysis platform was used to compare our ARDS data with (pre-analysed) publicly available transcriptomics data.

Statistical analysis

For each dataset analysed an appropriate linear mixed model was fitted. When required the data were logarithmically transformed to meet the assumptions of the analysis i.e. normally distributed errors and homogeneity of variance. Correction for false discovery rates in the transcriptional and cytokine analysis was according to the method of Benjamini and Hochberg [33]. The analyses were conducted in SAS version 9.3. Results are presented as

means ± SEM of (n) independent experiments, with p<0.05 considered statistically significant. Full details of the number of patients and HVs included in each assay are provided in **Suppl Figure S1.**

RESULTS

ARDS patient characteristics

Twenty-three mechanically ventilated patients fulfilling the 2011 Berlin definition for ARDS were recruited; their clinical, demographic and physiological characteristics are outlined in **Table 1**. Standardized ventilator strategies, in accordance with the ARDS Network low tidal volume protocol, were employed. At sample collection, 4/23 had severe ARDS (PaO_2/FiO_2 ratio ≤100 mmHg), 11/23 moderate ARDS (PaO_2/FiO2 ratio 101-200 mmHg) and 8/23 mild ARDS (PaO_2/FiO_2 ratio 201-300 mmHg). Sepsis and pneumonia were the commonest precipitating insults; 13 of 23 patients survived to discharge. All patients underwent FOB within 48 hours of diagnosis. PMNs constituted 69.7±4.2% of the differential leukocyte count in ARDS BALF (6.5±3.2% in control BALF) (**Table 1**). PMN abundance in BALF did not correlate with initial ARDS severity, abnormalities in gas exchange or BALF protein concentration (data not shown).

ARDS PMNs are phenotypically distinct

Comparing purified HV [blood]PMNs, ARDS [blood]PMNs and [alv]PMNs revealed striking differences in cell morphology. While HV [blood]PMNs had few hyper-segmented PMNs, [alv]ARDS PMNs displayed abundant hyper-segmented nuclei and cytoplasmic vacuolation (**Figure 1A**); hyper-segmented PMNs were not identified in control BALF. Immature 'band' PMNs were also more common in ARDS [blood]PMNs and [alv]PMNs (**Figure 1A**).

PMN activation status was assessed by confocal imaging of F-actin and cell surface staining of CD62L (L-selectin) and CD11b (Mac1). Prominent circumferential F-actin fluorescence was observed in a substantial proportion of the ARDS [blood]PMNs compared with HV [blood]PMNs (**Figure 1B**). The profile of surface receptor expression (up-regulation of CD11b and down-regulation of CD62L [36-37]) on both ARDS [blood]PMNs and [alv]PMNs is consistent with a primed and/or activated phenotype (**Figure 1C**).

ARDS blood and alveolar PMNs show delayed apoptosis and primed NADPH oxidase responses

Consistent with a previous report [23], we demonstrate that after 20 hours *ex-vivo* incubation, ARDS [alv]PMNs and [blood]PMNs demonstrated a significantly reduced number of apoptotic cells ($28.5 \pm 19.2\%$ (% apoptosis ± SEM) and $42.7 \pm 23\%$ respectively) compared to PMNs isolated from HV blood ($69.2 \pm 12\%$) (**Figure 2A**). The magnitude of the survival response exhibited by ARDS PMNs was equivalent ($28.6 \pm 10\%$) to the cytoprotective effect conferred by incubating HV [blood]PMNs with a maximally-effective concentration of rhGM-CSF (1 ng/ml) (data not shown).

We next compared the ability of ARDS [alv]PMNs and [blood]PMNs to mount an oxidative burst in response to fMLP, opsonized zymosan and *Streptococcus pneumoniae* (**Figure 2B-D**). In contrast to un-primed HV [blood]PMNs, which display minimal ROS generation to fMLP (**Figure 2B-C**), [alv]PMNs and [blood]PMNs from ARDS patients displayed robust ROS generation to all three stimuli, which in certain individuals exceeded those of TNFα-primed HV [blood]PMNs (**Figure 2D**). These data indicate basal priming and preserved NADPH oxidase responses of ARDS [alv]PMNs and [blood]PMNs, challenging the notion that inflammatory PMNs become 'exhausted' at peripheral sites.

ARDS blood and alveolar PMNs have preserved capacity for phagocytosis and NET formation

Previous investigators have identified a defect in the phagocytic and microbicidal activity of neutrophils from ARDS patients [38]. However, in our cohort, flow cytometry and confocal microscopy demonstrated that the capacity of ARDS ^{alv}PMNs and ^{blood}PMNs to phagocytose pHrodo™ RED-labelled *Staphylococcus aureus* was fully preserved (**Figure 3A-B**). This assay, supported by live cell imaging, is based on differential fluorescence of this bioparticle in an acidic environment, ensuring that only organisms within functional phagosomes are detected.

In addition to phagocytosis and the oxidative burst, PMNs deploy NETs to facilitate pathogen clearance. NETs are composed principally of a DNA scaffold decorated with anti-microbial granule proteins, which acts as a mesh to immobilize pathogens (**Figure 3C**). In response to PMA (**Figure 3 C-D**) or pyocyanin (data not shown) ARDS ^{alv}PMNs and ^{blood}PMNs displayed a similar capacity for NET production compared to HV ^{blood}PMNs. Collectively, our results, demonstrate preservation of the anti-microbial functions of ARDS ^{alv}PMNs and ^{blood}PMNs.

Defining the impact of ARDS on serum/BALF cytokine profiles and the transcriptional signatures of blood PMNs

To address whether factors present in the serum or BALF in ARDS patients could account for the primed/pro-survival PMN phenotype, a series of multiplex ELISA and bioassays were used to characterize the cytokine and growth factor profiles (n=18). As shown in **Figure 4** and **Suppl Figure S2**, a consistent profile of raised acute phase markers (e.g. CRP, SAA) and

inflammatory cytokines (e.g. TNFα, TARC, MCP-1, IL-8 and IL-6) was observed in ARDS serum and BALF compared to HV samples. By contrast, when BALF samples were corrected for total protein concentration, only CRP, IL-6 and MCP-1 levels were significantly higher in ARDS compared to control (**Suppl Figure S2**). Of note, at the single time point sampled, GM-CSF was only quantifiable in 5/23 ARDS BALF samples (LLoQ 7.6 pg/ml).

RNA transcriptomic analysis comparing freshly isolated ARDS [blood]PMNs with HV [blood]PMNs revealed a total of 1319 altered genes (using cut-offs of fold-change >1.5 and p<0.05; top ranked up- and down-regulated transcripts shown in **Figure 5A**; full list of all 1319 genes and their relative fold changes in **Suppl Table S3**). Using NextBio (which recognised 1282 of the 1319 differentially expressed genes) we compared these changes to publically available datasets, revealing a striking similarity to data in leukocytes from patients with severe burns or sepsis [39-40]; not only was there a strong overlap in gene changes, but also the direction of change correlated almost completely (**Figure 5B**). Ingenuity analysis revealed a significant increase in pathways associated with the immune response, cytoskeletal remodelling and mucin production, as well as significant decreases in cell death/apoptosis pathways, consistent with the neutrophil phenotype observed (**Suppl Figure S3**). Of note, of the 1319 observed transcript changes, only 216 were differentially expressed in the same direction compared to HV [blood]PMNs treated *ex-vivo* with GM-CSF (**Suppl Figure S4**). The data discussed in this publication have been deposited in NCBI's Gene Expression Omnibus and are accessible through GEO Series accession number GSE76293 (https://www.ncbi.nlm.nih.gov/geo/query/acc.cgi?acc=GSE76293).

Influence of the local airway environment on the ARDS PMN phenotype

To establish the significance of the alveolar inflammatory environment, we sought to induce a phenotypic switch using ARDS BALF. Incubating HV [blood]PMNs with IMDM+10% autologous serum containing ARDS BALF (50:50, v/v) reduced the extent of apoptosis observed *ex-vivo* at 20 hours ($37.4 \pm 21.7\%$ compared to 50:50, v/v control BALF $70.5 \pm 12.4\%$) (**Figure 6A**). Furthermore, treatment with ARDS BALF (50:50, v/v) for 30 minutes enhanced fMLP-induced ROS production in HV [blood]PMNs (**Figure 6B**), to a level comparable to optimally TNFα- or GM-CSF-primed HV [blood]PMNs (not shown), whilst control BALF had little effect. Thus ARDS BALF supernatant recapitulated the pro-survival, primed-NADPH oxidase signature seen in ARDS [blood/alv]PMNs.

Potential role of PI3K inhibition as a strategy to modulate ARDS [blood/alv] PMN behaviour

A key objective of this study was to define the sensitivity of inflammatory PMNs to PI3K inhibition, since this pathway is pivotal in neutrophil survival, priming/activation and reactive oxygen species (ROS) production [30]. Firstly, we confirmed that a pan-PI3K inhibitor ZSTK474 (10 µM) [41], and to a lesser extent the p38MAPK inhibitor SB741445 (10 µM) blocked GM-CSF-induced PMN survival in HV [blood]PMNs *in vitro* (**Figure 7A**). ZSTK474 also blocked the survival effect of ARDS BALF supernatant on HV [blood]PMNs (**Figure 7B**). However, neither compound restored normal neutrophil apoptosis in ARDS [blood]PMNs (**Figure 7C**) implying that the aberrant disease-associated neutrophil survival is either irreversible or operates through a PI3K-independent pathway. Given that even the delayed addition of ZSTK474 to GM-CSF-treated HV [blood]PMNs retains effectiveness in overcoming the pro-survival effect of this cytokine (data not shown), the involvement of a PI3K-independent pathway seems most likely. This conclusion is supported by the minimal overlap we observed between the transcriptomal signatures seen in the ARDS [blood]PMNs and those seen in HV [blood]PMNs treated with ZSTK474 (**Suppl Figure S5**). In contrast, ROS

production by PMNs from HV and ARDS patients was completely abrogated by ZSTK474 (**Figure 7D**).

DISCUSSION

Isoform-selective PI3K inhibitors have been proposed as anti-inflammatory agents in diseases such as ARDS [42], hence it is of importance to study their efficacy in patient-derived cells. ARDS [alv]PMNs have been little studied due to the difficulty of obtaining these cells from acutely unwell patients. Using purified blood and alveolar neutrophils from 23 ARDS patients, we demonstrate a stepwise change from HV [blood]PMNs through ARDS [blood]PMNs to ARDS [alv]PMNs. ARDS [alv]PMNs, and to a lesser extent ARDS [blood]PMNs, were distinct from HV [blood]PMNs, with hyper-segmented nuclei, increased CD11b expression, prolonged survival, and primed NADPH oxidase responses. Surprisingly, whilst the respiratory burst remained fully sensitive to PI3K inhibition, the pro-survival phenotype was not reversed by this strategy.

Few previous studies have assessed the characteristics of paired circulating and post-migrated inflammatory tissue neutrophils. The hyper-segmented CD11b^{high}/CD62L^{low} cells with enhanced oxidative capacity we identify in ARDS[blood] and ARDS [alv]PMNs are reminiscent of circulating neutrophils isolated following endotoxin challenge [43-44]; these latter cells were immunosuppressive, inhibiting T cell proliferation by release of hydrogen peroxide at the neutrophil/T cell interface. Increased nuclear segmentation and oxidative potential has also been observed in tumor-associated neutrophils (45), associated with increased anti-tumor activity. Prolonged survival of ARDS [alv]PMNs has been reported previously and attributed to GM-CSF/G-CSF in BALF [23], but in contrast to Matute-Bello *et al* we did not observe significantly elevated levels of these cytokines, perhaps related to disease heterogeneity and

differences in sampling time. Delayed apoptosis has been measured in neutrophils recruited to skin chambers versus paired circulating neutrophils, but synovial fluid-derived PMNs from patients with rheumatoid arthritis exhibited normal apoptosis [46]. These differences correlated with local IL1-β levels, but IL1-β in our ARDS BALF fluid was not significantly elevated. The variable functional capacity of neutrophils from different locations underscores the need to explore the efficacy of potential therapeutic agents in disease-relevant cell populations.

We observed a pro-inflammatory cytokine profile in the blood of ARDS patients, including several established priming agents. In our study, ARDS [blood] and ARDS [alv]PMNs were functionally primed, and such cells have been implicated in lung injury [47-48]. We previously demonstrated that the pulmonary capillary bed can trap and 'de-prime' neutrophils, and that this mechanism may fail in ARDS, augmenting the circulating pool of these potentially injurious cells [49]. Additional priming signals may be imparted during vascular transmigration [50], and ARDS BALF also primed the oxidative burst of HV [blood]PMNs. Thus a number of different factors may contribute to the pooling of primed neutrophils within the alveolar environment in ARDS.

ARDS [blood]PMNs and in particular ARDS [alv]PMNs survived longer during *ex-vivo* culture than HV [blood]PMNs. This pro-survival phenotype was recapitulated by incubating HV [blood]PMNs with ARDS BALF, implying that the enhanced longevity of these cells results at least in part from local exposure to mediators. However, whilst the pan-PI3K inhibitor ZSTK474 did not reduce the lifespan of ARDS [blood]PMNs it did reverse the pro-survival effects of both GM-CSF and BALF on HV [blood]PMNs in culture, suggesting that the complex cytokine environment in BALF is not the only factor conferring PI3K-resistance. It is

possible that the duration of exposure to pro-survival mediators *in vivo* prior to inhibitor exposure is relevant, and survival signals imparted during transmigration will likewise have been entrained prior to PI3K inhibition. Finally, hypoxia may impart additional signals that are also relatively PI3K-resistant, and HIF-dependent signalling was up-regulated (see **Suppl Table 3** - ranked 14th in the pathways changed in this setting). Together with the limited overlap between the ZSTK474 [blood]PMN or GM-CSF-[blood]PMN transcriptomes and the ARDS [blood]PMN signature, our results suggest that targeting of PI3K during ARDS, while suppressing the damaging ROS formation, would not enhance cell clearance via apoptotic pathways.

We further interrogated the activation state of ARDS [blood]PMNs by undertaking the first reported transcriptomic analysis of purified peripheral blood PMNs from ARDS patients. Our data revealed remarkable overlap between the transcriptomic profile of ARDS [blood]PMNs and those published for mixed leukocytes in burns (see **Figure 4B**) and sepsis cohorts [34-35]. The top five canonical pathways identified in the ARDS blood neutrophil gene signature were the glucocorticoid, IL-4, p38 MAPK, antigen presentation and CDC52 pathways. These were also within the top five pathways identified in the previous burns and sepsis cohorts using mixed leukocytes [39-40]. This suggests that despite their heterogeneity, there is a strong commonalty in a range of acute severe inflammatory disorders. This also provides possible directions for novel therapeutic interventions aimed for example at the IL-4 receptor or p38 pathways.

In this study we sought to characterise the functional and transcriptional profile of PMNs isolated from ARDS patients' blood and airways. Although our study captured only 23 patients at a single time point, our data add considerably to knowledge of [alv]PMN and

^{blood}PMN function and signaling profiles in ARDS; they challenge data from both animal models and from healthy cells, with a marked primed and pro-survival phenotype, the latter recalcitrant to PI3K inhibition. We conclude that intervention with a PI3K inhibitor in these patients is unlikely to be an effective therapeutic strategy, since it will impair PMN bactericidal function without facilitating inflammation resolution. Our findings highlight the importance of working with patient-derived cells, particularly for biomedical research into novel treatments for ARDS.

REFERENCES

1. Ashbaugh DG, Bigelow DB, Petty TL, Levine BE. Acute respiratory distress in adults. *Lancet* 1967;290:319-323.
2. Herridge, MS, Tansey CM, Matte A, Tomlinson G, Diaz-Granados N, Cooper A, Guest CB, Mazer CD, Mehta S, Stewart TE, Kudlow P, Cook D, Slutsky AS, Cheung AM. Functional disability 5 years after acute respiratory distress syndrome. *N Engl J Med* 2011;364:1293-1304.
3. Amato MBP, Barbas CSV, Medeiros DM, Magaldi RB, Schettino GP, Lorenzo-Filho G, Kairalla RA, Deheinzelin D, Munoz C, Oliveira R, Takagake TY, Carvalho RR. Effect of a protective-ventilation strategy on mortality in the acute respiratory distress syndrome. *N Engl J Med* 1998;338:347-354.
4. Thille AW, Esteban A, Fernandez-Segoviano P, Rodriguez JM, Aramburu JA, Vargas-Errazuriz P, Martin-Pellicer A, Lorente JA, Frutos-Vivar F. Chronology of histological lesions in acute respiratory distress syndrome with diffuse alveolar damage: a prospective cohort study of clinical autopsies. *Lancet Respir Med* 2013;1:395-401.
5. Weiland JE, Davis BW, Holter JF, Mohammed JR, Dorinsky PM, Gadek. Lung neutrophils in the adult respiratory distress syndrome. *Am Rev Respir Dis* 1986;133;218-225.
6. Matute-Bello G, Frevert CW, Martin TR. Animal models of acute lung injury. *Am J Physiol Lung Cell Mol Physiol* 2008;295;379-399.
7. Pillay J, den Braber I, Vrisekoop N, Kwast LM, de Boer RJ, Borghans JA, Tesselaar K, Koenderman L. In vivo labeling with ^2H_2O reveals a human neutrophil lifespan of 5.4 days. *Blood* 2010;116:625-627.
8. Pillay J, Kamp VM, van Hoffen E, et al. A subset of neutrophils in human systemic inflammation inhibits T cell responses through Mac-1. *J Clin Invest* 2012;122:327-336.
9. Abadie V, Badell E, Douillard P, Ensergueix D, Leenen PJ, Tanguy M, Fiette L, Saeland S, Gicquel B, Winter N. Neutrophils rapidly migrate via lymphatics after Mycobacterium bovis BCG intradermal vaccination and shuttle live bacilli to the draining lymph nodes. *Blood* 2005;106:1843-1850.
10. Beauvillain C, Delneste Y, Scote M, Peres A, Gascan H, Guermonprez P, Barnaba V, Jeannin P. Neutrophils efficiently cross-prime naive T cells in vivo. *Blood* 2007;110:2965-2973.
11. Gosselin EJ, Wardwell K, Rigby WF, Guyre PM. Induction of MHC class II on human polymorphonuclear neutrophils by granulocyte/macrophage colony-stimulating factor, IFN-gamma, and IL-3. *J Immunol* 1993;151:1482-1490.
12. Woodfin A, Voisin MB, Beyrau M, Colom B, Caille D, Diapouli FM, Nash GB, Chavakis T, Albelda SM, Rainger GE, Meda P, Imhof BA, Nourshargh S. The junctional adhesion molecule JAM-C regulates polarized transendothelial migration of neutrophils in vivo. *Nat Immunol* 2011;12:761-769.
13. Lakschevitz FS, Visser MB, Sun C, Glogauer M The following reference has now been included: Neutrophil transcriptional profile changes during transit from bone marrow to sites of inflammation. *Cell Mol Immunol* 2015;12:53-65.
14. Desai AA, Hysi P, Garcia JGN. Integrating genomic and clinical medicine: searching for susceptibility genes in complex lung disease. *Translational Research* 2007;151;181-193.
15. Yamamoto K, Ahyi AN, Pepper-Cunningham Z, Ferrari JD, Wilson AA, Jones MR, Quinton LJ, Mizgerd JP. Roles of lung epithelium in neutrophil recruitment during pneumococcal pneumonia. *Am J Respir Cell Mol Biol* 2014;50:253-262.

16. Ballinger MN, Paine R, Serezani CH, Aronoff DM, Choi ES, Standiford, Toews, Moore BB. Role of granulocyte macrophage-stimulating factor during gram-negative lung infection with Pseudomonas aeruginosa. *Am J Respir Cell Mol Biol* 2006;34:766-774.

17. LeVine AM, Reed JA, Kurak KE, Cianciolo E, Whitsett JA. GM-CSF-deficient mice are susceptible to pulmonary group B streptococcal infection. *J Clin Invest* 1999;103:563-569.

18. Suzuki T, Sakagami T, Young LR, Carey BC, Wood RE, Zimmerman SL, Smolarek T, Dishop MK, Wert SE, Whitsett JA, Grabowski G, Carey, Stevens C, van der Loo JC, Trapnell BC. Familial pulmonary alveolar proteinosis caused by mutations in CSF2RA. *J Exp Med* 2008;205:2703-2710.

19. Kitamura T, Tanaka N, Watanabe J, Uchida S, Idiopathic pulmonary alveolar proteinosis as an autoimmune disease with neutralizing antibody against granulocyte/macrophage colony-stimulating factor. *J Exp Med* 1999;190:875-880.

20. McColl SR, Beauseigle D, Gilbert C, Naccache PH. Priming of the human neutrophil respiratory burst by granulocyte-macrophage colony-stimulating factor and tumor necrosis factor-alpha involves regulation at a post-cell surface receptor level. Enhancement of the effect of agents with directly activate G proteins. *J Immunol* 1990;145-3047-3053.

21. Juss JK, Hayhoe RP, Owen CE, Bruce I, Walmsley SR, Cowburn AS, Kulkarni S, Boyle KB, Stephens L, Hawkins PT, Chilvers ER, Condliffe AM. Functional redundancy of class I phosphoinositide 3-kinase (PI3K) isoforms in signaling growth factor-mediated human neutrophil survival. *PLoSOne* 2012;7:e45933.

22. Frossard JL, Saluja AK, Mach N. In vivo evidence for the role of GM-CSF as a mediator in acute pancreatitis-associated lung injury. *Am J Physiol-Lung Cell Mol Physiol* 2002;3:L541-L538.

23. Matute-Bello G, Liles WC, Radella F, Steinberg KP, Ruzinske JT, Jonas M, Chi EY, Hudson LD, Martin TR. Neutrophil apoptosis in the acute respiratory distress syndrome. *Am J Respir Crit Care Med.* 1997;156:969-977.

24. Chen C, Fang X, Wang Y, Li Y, Wang D, Zhao X, Bai C, Wang X. Preventative and therapeutic effects of phosphoinositide 3-kinase inhibitors on acute lung injury. *Chest* 2011;140;391-400.

25. Kim Di, Kim SR, Kim HJ, Lee SJ, Park SJ, Im MJ, Lee YC. PI3K-γ inhibition ameliorates acute lung injury through regulation of IκBα/NF-κB pathway and innate immune responses. *J Clin Immunol* 2012;32:340-351.

26. Hamers L, Kox M, Pickkers P. Sepsis-induced immunoparalysis: mechanisms, markers, and treatment options. *Minerva Anestesiol* 2015;81:426-439.

27. Morris AC, Kefala K, Wilkinson TS, Shaliwal K, Farrell L, Walsh T, MacKenzie SJ, Reid H, Davidson DJ, Haslett C, Rossi AG, Sallenave JM, Simpson JA. C5a-mediated neutrophil dysfunction is RhoA-dependent and predicts infection in critically ill patients. *Blood* 2009;117:5178-5188.

28. Juss J, Herre J, Begg M, Bradley G, Lennon M, Amour A, House D, Hessel EM, Summers C, Condliffe AM, Chilvers ER. Genome-wide transcription profiling in neutrophils in acute respiratory distress syndrome. *Lancet* 2015;385 Suppl 1:S55.

29. ARDS Definition Task Force. Ranieri VM, Rubenfeld GD, Thompson BT, Ferguson ND, Caldwell E. Acute respiratory distress syndrome: the Berlin Definition. *JAMA* 2012;307:2526-2533.

30. Cowburn AS, Summers C, Dunmore BJ, Farahi N, Hayhoe RP, Print CG, Cook SJ, Chilvers ER. Granulocyte/macrophage colony-stimulating factor causes a paradoxical increase in the BH3-only pro-apoptotic protein Bim in human neutrophils. *Am J Respir Cell Mol Biol* 2011;44:879-887.

31. Bain, B. Bloods cells. A practical guide. 4th edition. Oxford: Blackwell Publishing; 2006.
32. Irizarry RA, Hobbs B, Collin F, Beazer-Barclay YD, Antonellis KJ, Scherf U, Speed TP. Exploration, normalization, and summaries of high density oligonucleotide array probe level data. *Biostatistics* 2003;4:249-264.
33. Benjamini Y, Hochberg Y. Controlling the false discovery rate: A practical and powerful approach to multiple testing. *J Royal Stat Soc* B 1995;57:289-300.
34. Condliffe AM, Davidson K, Anderson K, Ellson CD, Crabbe T, Okkenhaug K, Vanhaesebroeck B, Turner M, Webb L, Wymann MP, Hirsch E, Ruckle T, Camps M, Rommel C, Jackson SP, Chilvers ER, Stephens LR, Hawkins PT. Sequential activation of class IB and class IA PI3K is important for the primed respiratory burst of human but not murine neutrophils. *Blood* 2005;106:1432-1440.
35. Benjamini Y and Hochberg Y. Controlling the False Discovery Rate: A Practical and Powerful Approach to Multiple Testing. *J Royal Stat Soc* 1995;57:289-300.
36. Ley K, Gaehtgens P, Fennie C, Singer MS, Lasky LA, Rosen SD. Lectin-like cell adhesion molecule 1 mediates leukocyte rolling in mesenteric venules in vivo. *Blood* 1991;77:2553-2555.
37. Fortunati E, Kazemier KM, Grutters JC, Koenderman L, Van den Bosch van JMM. Human Neutrophils Switch to an Activated Phenotype after Homing to the Lung Irrespective of Inflammatory Disease. *Clin Ex Immunol* 2009;155:559-566.
38. Mascellino MT, Delogu G, Pelaia MR, Ponzo R, Parrinello R, Giardina A. Reduced bactericidal activity against Staphylococcus aureus and Pseudomonas aeruginosa of blood neutrophils from patients with early adult respiratory distress syndrome. *J Med Microbiol* 2001;50:49-54.
39. Zhou B1, Xu W, Herndon D, Tompkins R, Davis R, Xiao W, Wong WH; Inflammation and Host Response to Injury Program, Toner M, Warren HS, Schoenfeld DA, Rahme L, McDonald-Smith GP, Hayden D, Mason P, Fagan S, Yu YM, Cobb JP, Remick DG, Mannick JA, Lederer JA, Gamelli RL, Silver GM, West MA, Shapiro MB, Smith R, Camp DG 2nd, Qian W, Storey J, Mindrinos M, Tibshirani R, Lowry S, Calvano S, Chaudry I, West MA, Cohen M, Moore EE, Johnson J, Moldawer LL, Baker HV, Efron PA, Balis UG, Billiar TR, Ochoa JB, Sperry JL, Miller-Graziano CL, De AK, Bankey PE, Finnerty CC, Jeschke MG, Minei JP, Arnoldo BD, Hunt JL, Horton J, Cobb JP, Brownstein B, Freeman B, Maier RV, Nathens AB, Cuschieri J, Gibran N, Klein M, O'Keefe G. Analysis of factorial time-course microarrays with application to a clinical study of burn injury. *Proc Natl Acad Sci USA* 2010;107:9923-9928.
40. Sutherland A, Thomas M, Brandon RA, Brandon RB, Lipman J, Tang B, McLean A, Pascoe R, Price G, Nguyen T, Stone G, Venter D. Development and validation of a novel molecular biomarker diagnostic test for the early detection of sepsis. *Crit Care* 2011;15:R149.
41. Yaguchi S, Fukui Y, Koshimizu I, Yoshimi H, Matsuno T, Gouda H, Hirono, S, Kanami Y, Yamori T. Antitumor activity of ZSTK474, a new phosphatidylinositol 3-kinase inhibitor. *J Nat Cancer Inst* 2006;98:545-556.
42. Crabbe T, Welham MJ, Ward SG. The PI3K inhibitor arsenal: choose your weapon! *Trends Biochem Sci* 2007;32:450-456.
43. Scapini P, Cassatella MA. Social networking of human neutrophils within the immune system. *Blood* 2014;124:710-719.
44. Pillay J, Ramakers BP, Kamp VM, Loi AL, Hietbrink F, Leenen LP, Tool AT, Picckers P, Koenderman L. Functional heterogeneity and differential priming of circulating neutrophils in human experimental endotoxemia. *J Leukoc Biol* 2010;88:211-220.

45. Fridlender ZG, Sun J, Kim S, Kapoor V, Cheng G, Ling L, Worthen GS, Albelda SM Polarization of tumor-associated neutrophil phenotype by TGF-beta: "N1" versus "N2" TAN. *Cancer Cell* 2009;16:183-194.

46. Christenson K, Björkman L, Karlsson A, Bylund J. Regulation of neutrophil apoptosis differs after in vivo transmigration to skin chambers and synovial fluid: a role for inflammasome-dependent interleukin-1β release. *J Innate Immun* 2013;5:377-388.

47. Botha AJ, Moore FA, Moore EE, Kim FJ, Banerjee A, Peterson VM. Postinjury neutrophil priming and activation: an early vulnerable window. *Surgery* 1995;118:358-365.

48. Drost EM, MacNee W. Potential role of IL-8, platelet-activating factor and TNF-alpha in the sequestration of neutrophils in the lung: effects on neutrophil deformability, adhesion receptor expression and chemotaxis. *Eur J Immunol.* 2002;32:393-403.

49. Summers C, Singh NR, White JF, Mackenzie IM, Johnston A, Solanki C, Balan KK, Peters AM, Chilvers ER. Pulmonary retention of primed neutrophils: a novel protective host response, which is impaired in the acute respiratory distress syndrome. *Thorax* 2014;69:623-629.

50. Paulsson JM, Jacobson SH, Lundahl J. Neutrophil activation during transmigration in vivo and in vitro: A translational study using the skin chamber model. *J Immunol Methods* 2010;361:82-88.

FIGURE LEGENDS

Table 1

Clinical characteristics of patients with ARDS

Figure 1

Circulating and alveolar neutrophils from patients with ARDS are phenotypically distinct compared to healthy volunteer neutrophils

A. Morphology of freshly purified PMNs from HVs in comparison with ARDS blood and alveolar PMNs was assessed. Representative photomicrographs of cytospins (x100, stained with modified Wright stain) of HV ^{blood}PMNs, and autologous ^{alv}PMNs and ^{blood}ARDS PMNs isolated in parallel (n=19). Classical PMNs have 3-4 nuclear lobes connected by filaments of dense heterochromatin, band PMNs (red arrow) contain a curved nucleus that is not completely segmented into lobes, and hyper-segmented PMNs (black arrow) have nuclei comprised of five or more lobes. ARDS BALF contains abundant hyper-segmented PMNs with up to 12 nuclear lobes (inset). PMN subsets present in the blood (HV n=19; ARDS n=19) and ARDS BALF (n=11) were quantitated morphologically by light microscopy (right-hand panel). The %PMN subsets were analyzed on the $\log_{10}$ scale using a linear fixed effects model (*** $P<0.0001$ for hyper-segmented cells). **B**. HV ^{blood}PMNs and autologous ARDS ^{alv}PMNs and ^{blood}PMNs stained for F actin polarization (rhodamine-phalloidin – green) and elastase (red) with nuclei (DAPI) depicted in blue. Representative (of n=3) immunofluorescence confocal photomicrographs (x40) illustrate ARDS ^{alv}PMNs and ^{blood}PMNs display a prominent circumferential F actin ring (white arrows). **C**. PMN cell surface CD62L-FITC and CD11b-APC expression of freshly isolated HV ^{blood}PMNs, autologous ARDS ^{alv}PMNs and ^{blood}PMNs assessed by flow cytometry. Results are representative of three independent experiments. The CD11b expression (MFI corrected for

isotype control readings) for HV blood neutrophils was 11.7±0.9, ARDS blood neutrophils 74±6, and ARDS BALF neutrophils 427±50; the CD62L expression (MFI corrected for isotype control readings) for HV blood neutrophils 114±12, ARDS blood neutrophils 8.4±0.6, and ARDS BALF neutrophils 8.7±1.9.

Figure 2

Circulating and alveolar neutrophils from patients with ARDS exhibit delayed apoptosis and heterogeneous NADPH oxidase responses

A. HV [blood]PMNs (5×10^6/ml) were cultured in IMDM with 10% autologous serum. Apoptosis was quantitated by flow cytometry following AnV staining after 20 hours in culture. The data were analyzed using a linear fixed effects model (**P<0.001, ***P<0.0001). **B**. Representative kinetic profile of the neutrophil oxidative burst. Freshly purified HV [blood]PMNs (unprimed-black squares and rhTNFα (10 ng/ml), primed-white squares), autologous ARDS [alv]PMNs (black circles) and [blood]PMNs (white circles) were incubated with luminol and HRP in a 96-well luminometer plate and fMLP (100 nM) added via the injection port of a Centro LB 960 luminometer (Berthold Technologies); light emission (RLU) was recorded at 6 second intervals over 10 minutes. **C**. The oxidative response in freshly isolated un-primed and rhTNFα-primed HV blood following stimulation with fMLP is expressed as the relative peak height to the rhTNFα-primed response in HV [blood]PMNs. **D.** Peak height of the neutrophil oxidative response in freshly isolated autologous ARDS [alv]PMNs and [blood]PMNs normalised to the HV blood PMN response in **Di** to fMLP (100 nM), **Dii** to serum-opsonized zymosan (5-7 particles/PMN), and **Diii** to serum-opsonized heat-killed *Streptococcus pneumoniae* (5-7 particles/PMN).

Figure 3

Circulating and alveolar neutrophils from patients with ARDS exhibit preserved phagocytic capacity and heterogeneous NET responses

A. Analysis of phagocytosis by freshly isolated PMNs. Representative (of n = 5 experiments) immunofluorescence confocal photomicrographs taken after 1 hour incubation demonstrating internalized pHRodo conjugated *S. aureus* (red) and PMN nuclei counterstained with DAPI (blue). **B.** PMN phagocytosis was quantitated by flow cytometry with fluorescence excitation 530 nm/emission 590 nm. These data were analyzed using a linear fixed effect model (ns $p > 0.05$). **C.** NET formation by freshly isolated autologous blood and alveolar ARDS PMNs and HV PMNs was assessed following treatment with PMA (20 nM) or vehicle control. Representative (n=4) fluorescence photomicrographs of NETs, x63 magnification. Unmerged images (lower panels) stained for extracellular DNA scaffold (SYTOX: green) and citrullinated histones (CitHis: red). The precise overlap of these two colors in merged images generates the ochre color representing NETS in the PMA-treated cells; no NETS are visible in the control samples. **D.** Kinetics of NETs formation was assessed over 4 hours by measuring total fluorescence using a VICTOR[3] Multilabel Reader using Wallac 1420 Workstation v3.00 software and subtracting baseline fluorescence.

Figure 4

Heat map of the inflammatory markers in the serum of healthy volunteers and patients with ARDS

Inflammatory mediators in serum were measured using either an ELISA kit or an electrochemical luminescence immunoassay MesoScale Discovery (MSD) multiplex. In the heatmap each row is a different cytokine and each column is a different patient. The coloring represents the abundance of the inflammatory marker measured. The lowest abundance measured are presented by bright green while the highest by bright red. To assess the mean

difference in abundance between the disease groups a linear mixed model was fitted to the data with disease as a fixed effect and the donor pairing as a random effect. The heat maps and dendrogram (variable tree) were obtained from a hierarchical clustering of the cytokines using complete linkage. The variable tree to the left of the heat map shows how the cytokines cluster together based on their Pearson's correlation i.e., the more correlated two cytokines are the closer they are in the branches of the dendrogram. The stars on the plot represent the FDR adjusted p-value of the disease effect in this model where NS=FDR p>0.05, *=FDR p <0.05, **=FDR p< 0.001 and ***=FDR p< 0.0001.

Figure 5

Genes altered greater than 5-fold in ARDS blood neutrophils compared to healthy volunteer blood neutrophils

A. Negative values indicate a decrease in relative gene expression, while positive values indicate an increase in relative gene expression. All $p<0.05$ with (n) = 12 for ARDS and HV blood PMNs. **B.** Diagrammatic representation of gene transcript changes between ARDS and HV blood PMNs and the overlap in the ARDS transcript signature with pediatric early stage burn data [39].

Figure 6

Treatment of healthy volunteer blood neutrophils with BALF from patients with ARDS replicates the pro-survival and primed neutrophil phenotype

A. HV PMNs were incubated in IMDM+10% autologous serum containing either 50:50 v/v control BALF or ARDS BALF and apoptosis was assessed at 20 hours by flow cytometry following AnV staining. These data were analyzed using a linear mixed effects model with the HV donor fitted as a random effect (ns P>0.05, ***P<0.0001). **B.** Freshly isolated HV

PMNs were treated with 50:50 v/v control BALF or ARDS BALF for 30 minutes at 37°C prior to stimulation with fMLP (100 nM). Chemiluminescence was recorded using a Centro LB 960 luminometer and expressed graphically as the absolute peak height in relative light units (RLU). These data were analysed on the $\log_{10}$ scale using a linear mixed effects model with the HV donor fitted as a random effect (ns P>0.05, ***P<0.0001).

Figure 7

Effects of PI3K and p38 MAPK inhibition on healthy blood and ARDS neutrophils

A. HV blood PMNs were pre-incubated with either 0.1% DMSO vehicle control, p38 MAPK inhibitor (SB741445 (10 μM)) or pan-Class I PI3K inhibitor (ZSTK474 (10 μM)) for 20 mins and then treated with rhGM-CSF (1 ng/ml). Apoptosis was quantitated after 20 hours in culture by flow cytometry following AnV and PI staining. These data were analyzed using a linear mixed effects model with the HV donor fitted as a random effect (***P<0.0001). **B.** HV blood PMNs were pre-incubated with the indicated inhibitors for 20 mins prior to culture in 50:50 v/v ARDS BALF. Apoptosis was quantitated after 20 hours in culture by flow cytometry following AnV and PI staining. These data were analyzed using a linear mixed effects model with the HV donor fitted as a random effect (ns P>0.05, **P<0.001). **C.** ARDS blood PMNs were incubated with SB741445 or ZSTK474 and apoptosis was quantitated by flow cytometry following AnV and PI staining. These data were analyzed using a linear mixed effects model with the HV donor fitted as a random effect (ns P>0.05, *P<0.05). **D.** ARDS blood and alveolar PMNs were pre-incubated with ZSTK474 (10 μM) for 30 minutes at 37°C prior to stimulation with fMLP (100 nM). Chemiluminescence was recorded using a Centro LB 960 luminometer and expressed graphically as the absolute peak height in relative light units (RLU). Data were analysed on the $\log_{10}$ scale using a linear mixed effects model with the HV donor fitted as a random effect (* P<0.05, ***P<0.0001).

Table 1.   Demographics and clinical characteristics of patients with ARDS

	ARDS		
	Mild	**Moderate**	**Severe**
Number of patients	8	11	4
Mean age (years)	49±16.3	62.7±11.1	48.3±21.0
Gender (Male:Female)	7:1	5:6	3:1
Patient mortality (n)	2	7	2
PaO_2 (mmHg)	92.2±17.6	82.4±16.8	68.4±2.3
Mean PaO_2/FiO_2 (mmHg)	246.1±18.9	139.5±18.8	90.0±5.7
PEEP (cmH_2O)	8.9±2.1	8.9±2.6	8.5±1.9
Blood WBC	11.1±10.1	10.8±8.0	12.9±8.4
Blood PMN count	8.4±7.2	9.7±7.9	11.4±7.5
% PMNs in BALF	69.7±2 (n=6)	73.7±11.1 (n=10)	59.8±2 (n=3)
Etiology of ARDS	Community acquired pneumonia, neutropenic sepsis, fresh water drowning, liver failure post transplant donation, ethylene glycol poisoning	Community acquired pneumonia, aspiration pneumonia, neutropenic sepsis	Community acquired pneumonia, aspiration pneumonia, neutropenic sepsis

ARDS neutrophils have a distinct phenotype and are resistant to phosphoinositide 3-kinase inhibition

Juss JK, House D, Amour A, Begg M, Herre J, Storisteanu DML, Hoenderdos K, Bradley G, Lennon M, Summers C, Hessel EM, Condliffe AM, Chilvers ER.

<u>Online Data Supplement</u>

<u>Supplementary Figure 1</u>

Flowchart showing the precise details of the number of subjects included in each assay.

<u>Supplementary Figure 2</u>

Inflammatory markers in the BALF of patients with ARDS

The concentration of key inflammatory mediators, were measured in control (n = 10) and ARDS (n = 18) BALF supernatants either by ELISA kit or an electrochemical luminescence immunoassay MesoScale Discovery (MSD) multiplex. **S1(i)** shows a heatmap representation of BALF markers in control subjects (C01-C10) vs ARDS patients (A01-18) without correction for BALF total protein, and **S1(ii)** shows a heatmap representation of the identical samples after correction for BALF total protein content (* P<0.05, ** P<0.01, ***P<0.001).

<u>Supplementary Figure 3</u>

Heat map of the transcriptomic changes in HV and ARDS blood PMNs

A. Immune response. **B**. Apoptosis. **C**. Cytoskeletal remodelling. **D**. Mucin production. (n) = 12 for both groups.

Supplementary Figure 4

The genes altered greater than 5-fold in ARDS neutrophils compared to HV neutrophils

Negative values indicate a decrease in relative gene expression, while positive values indicate an increase in relative gene expression. Bars highlighted in red where also altered in HV PMNs incubated with GM-CSF (fold change>1.5, p<0.05, (n) = 12 for all groups).

Supplementary Figure 5

The genes altered greater than 5-fold in ARDS neutrophils compared to HV neutrophils
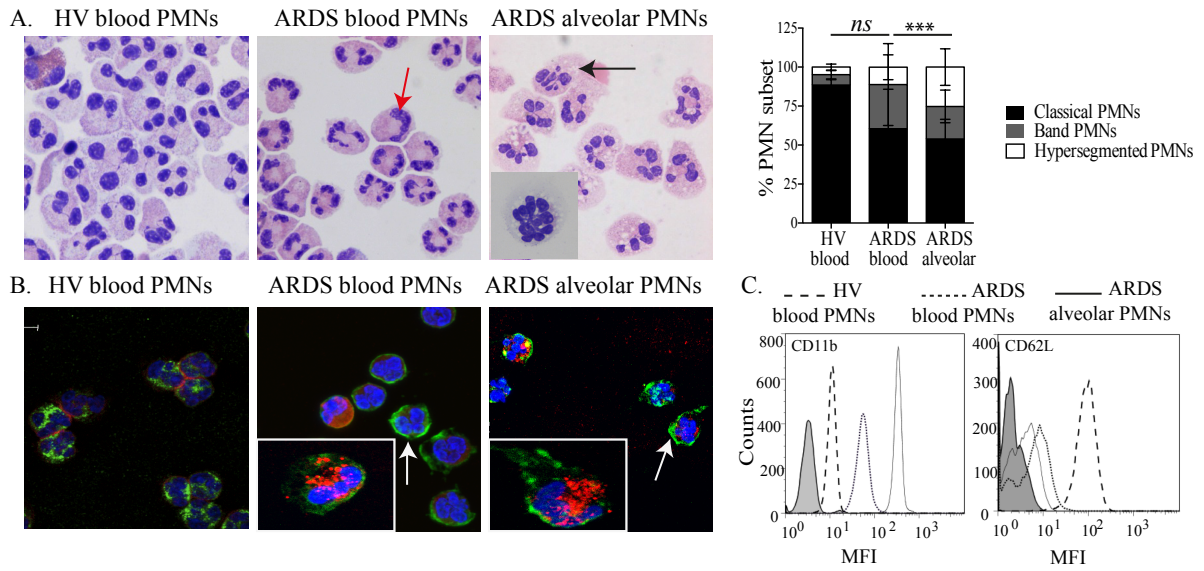
Negative values indicate a decrease in relative gene expression, while positive values indicate an increase in relative gene expression. Bars highlighted in green were also altered in HV PMNs incubated with a pan-PI3K inhibitor (fold change>1.5, p<0.05, (n) = 12 for all groups).
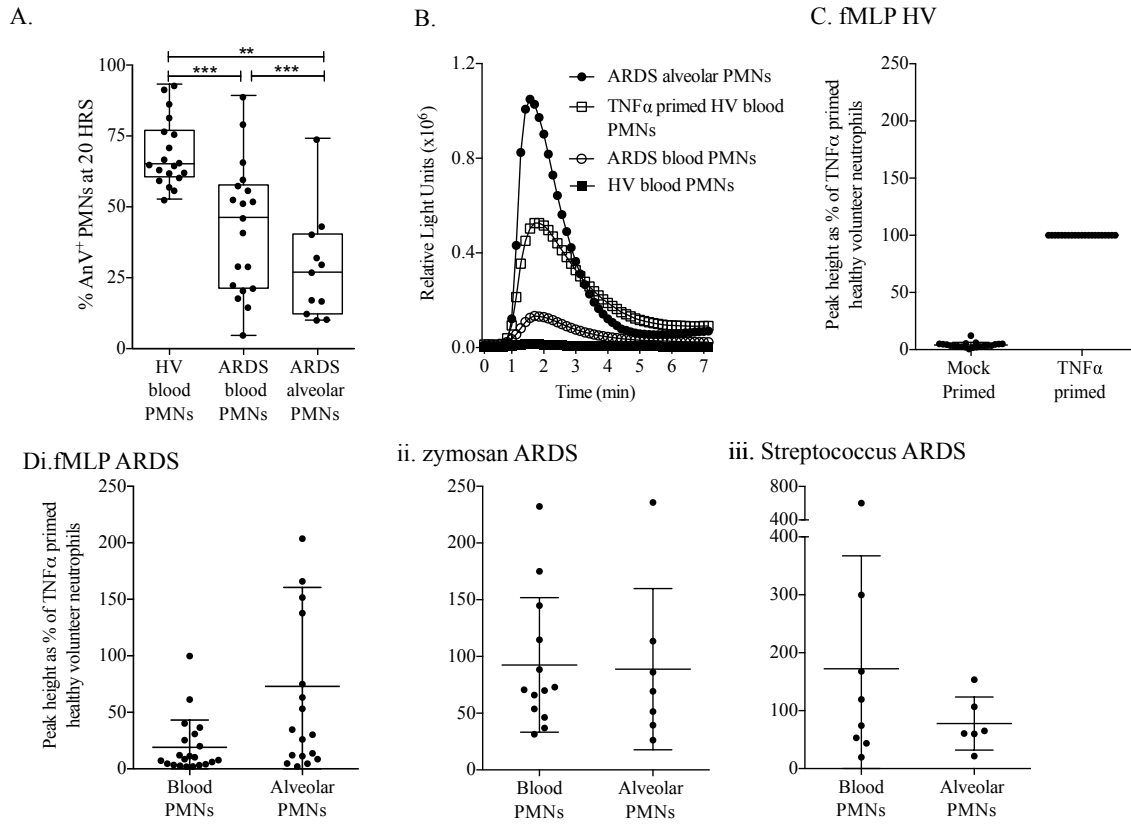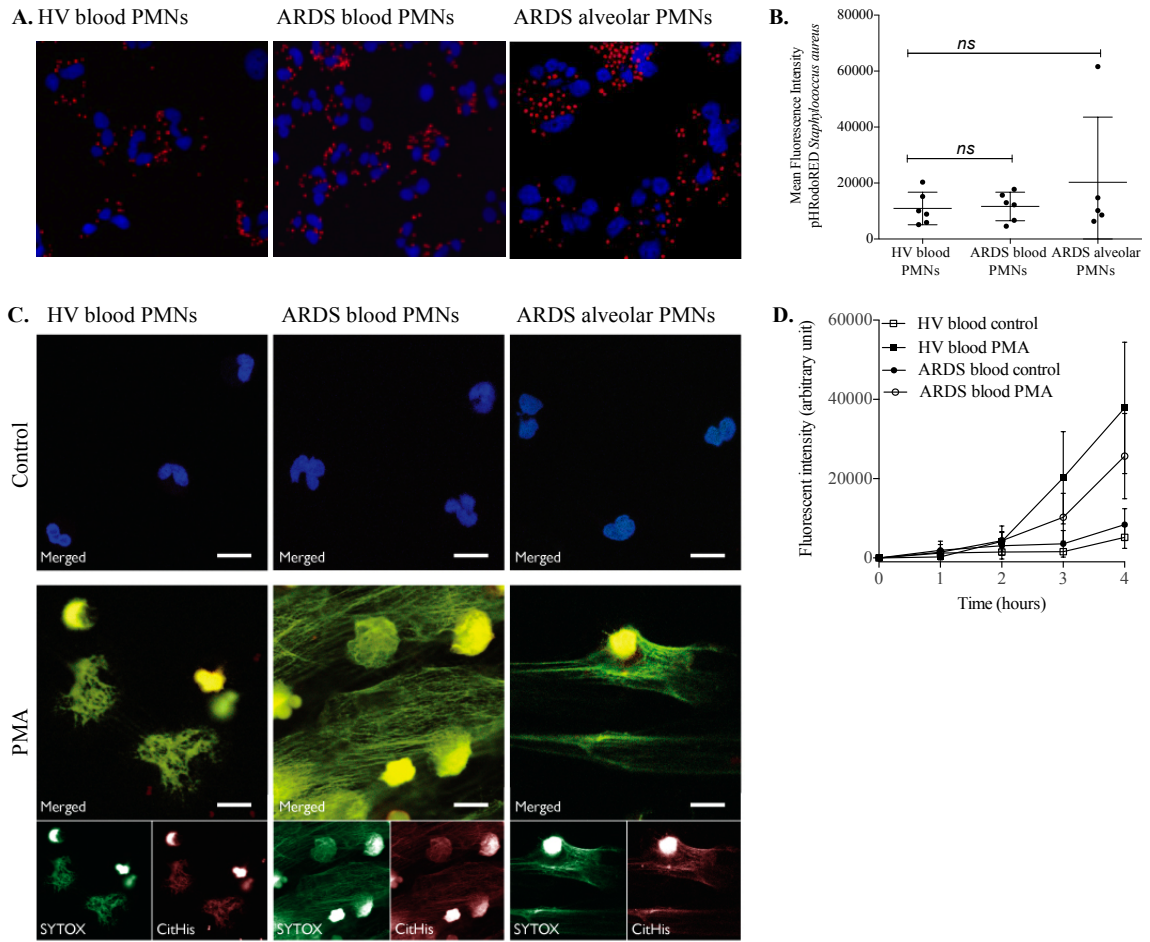
Supplementary Table 2

Tables (i)-(vi) provide the full data set for blood and BALF cytokine values for HVs and ARDS patients. For the BALF samples these are given both corrected and uncorrected for total protein content.

Supplementary Table 3

A comprehensive list of all 1319 significantly altered genes (fold change > 1.5; unadjusted p-value < 0.05; false discovery rate q-value < 0.05) identified by the comparison of freshly isolated ARDS [blood]PMNs with HV [blood]PMNs using Affymetrix mRNA transcriptomic analysis.

Juss et al. 2016
Figure 1

A.   HV blood PMNs   ARDS blood PMNs   ARDS alveolar PMNs

B.   HV blood PMNs   ARDS blood PMNs   ARDS alveolar PMNs

C.

A.

B.

C. fMLP HV

Di.fMLP ARDS

ii. zymosan ARDS

iii. Streptococcus ARDS

A. HV blood PMNs   ARDS blood PMNs   ARDS alveolar PMNs

B.

C. HV blood PMNs   ARDS blood PMNs   ARDS alveolar PMNs

D.

A.

B.

Juss et al. 2016
Figure 6

A.

B.

Control BALF (50:50)	-	+	-
ARDS BALF (50:50)	-	-	+

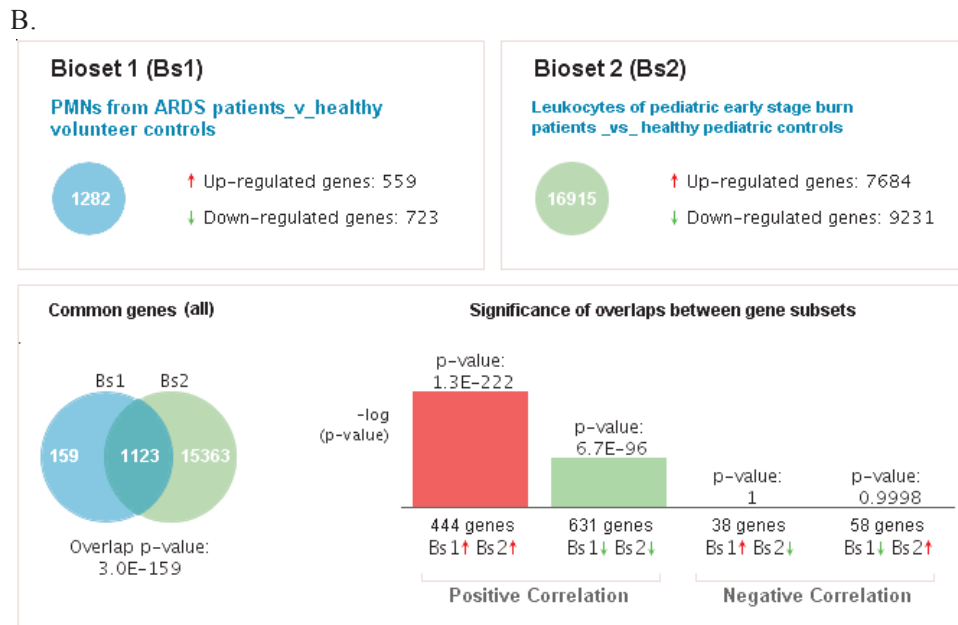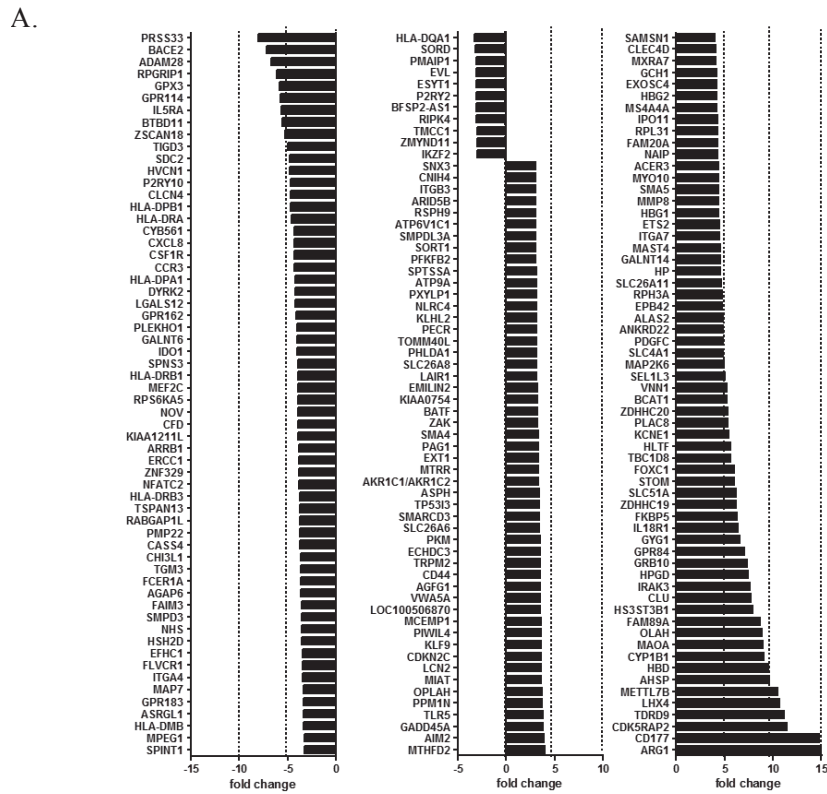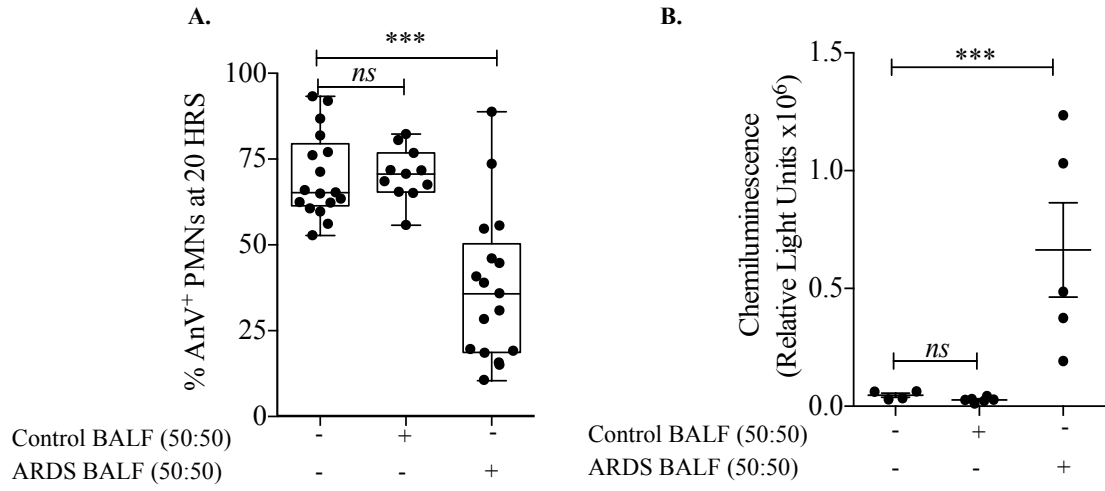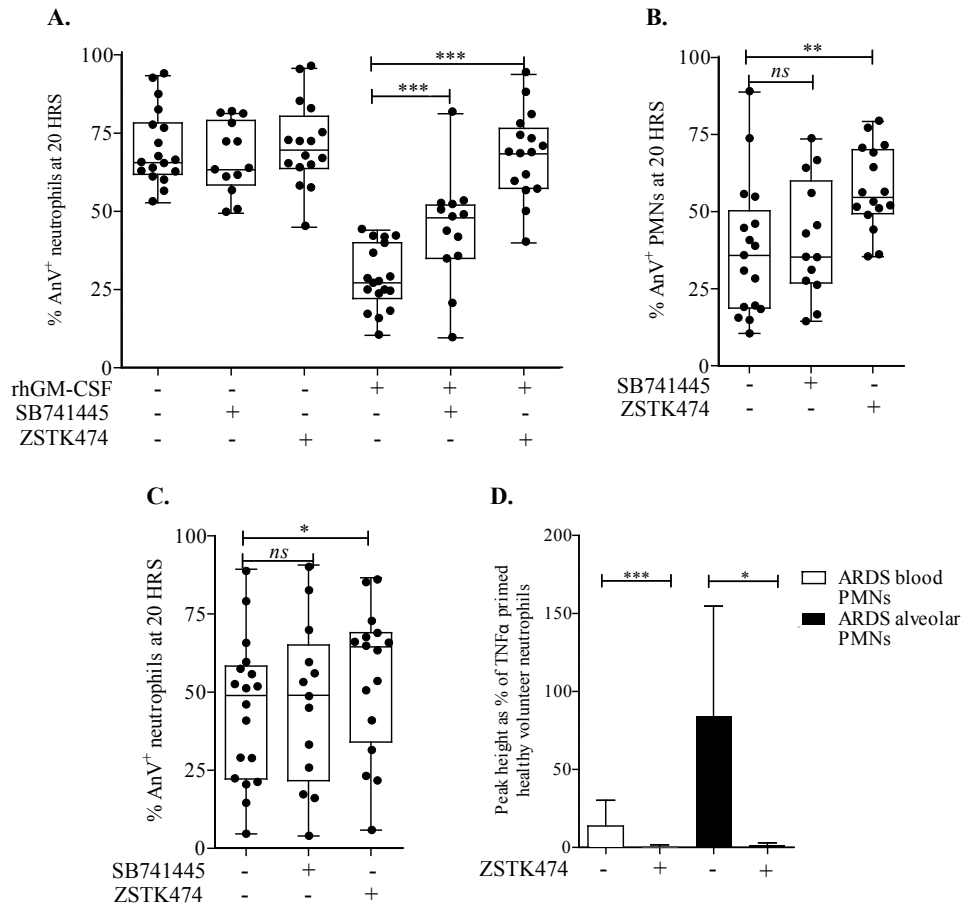|			
Control BALF (50:50)	-	+	-
ARDS BALF (50:50)	-	-	+

Juss et al. 2016
Figure 7

A.

B.

C.

D.

Supplementary Figure 1

HV Blood PMNs | ARDS Blood PMNs | ARDS Alveolar PMNs | HV Blood | Control BALF | ARDS BALF

Phenotype | Function | Mediators | Transcriptomics | Inhibitors

Figure 1
PMN subsets
HV blood (n=22)
ARDS blood (n=21)
ARDS alveolar (n=11)

F-actin & cell surface immunophenotype
Representative (n=3)

Figure 6
BALF apoptosis
Vehicle control (n=17)
Control BALF (n=11)
ARDS BALF (n=17)

BALF priming
Vehicle control (n=5)
Control BALF (n=5)
ARDS BALF (n=5)

Figure 2
PMN apoptosis
HV blood (n=19)
ARDS blood (n=19)
ARDS alveolar (n=11)

PMN ROS
a. fMLP
HV blood (n=21)
ARDS blood (n=21)
ARDS alveolar (n=18)

b. Zymosan
HV blood (n=13)
ARDS blood (n=13)
ARDS alveolar (n=7)

c. Streptococcus
HV blood (n=8)
ARDS blood (n=8)
ARDS alveolar (n=6)

Figure 3
Phagocytosis
HV blood (n=6)
ARDS blood (n=6)
ARDS alveolar (n=5)

NETs
HV blood (n=4)
ARDS blood (n=4)

Figure 4
Mediators
a. Serum
HV (n=18)
ARDS (n=18)

b. BALF
-Controls (n=10)
-ARDS (n=18)

Figures 5, S3A & S3B
ARDS gene signature
HV (t=0; n=12)
ARDS (t=0; n=12)

Figures S4 & S5
GM-CSF & PI3Ki signatures
HV (t= 6h; n=10)
(i) Vehicle
(ii) Pan-PI3K
(iii) GM-CSF
(iv) GM-CSF + PanPI3K

Figure 7
PI3K inhibitor data
a. Apoptosis
HV blood PMNs + ARDS BALF (n=16)
HV blood PMNs + ARDS BALF + PI3Ki (n=16)
HV blood PMNs+ ARDS BALF + p38i (n=14)

b. Apoptosis
ARDS blood PMNs (n=18)
ARDS blood PMNs+PI3K inhibitor (n=16)
ARDS blood PMNs+ MAPK inhibitor (n=13)

c. Apoptosis
HV blood PMNs + PI3K inhibitor (n=16) HV blood PMNs + MAPK inhibitor (n=13)

ROS + PI3K
a. ARDS blood PMNs + PI3K (n=12)
b. ARDS alveolar PMNs + PI3K (n=4)

(i)

(ii)
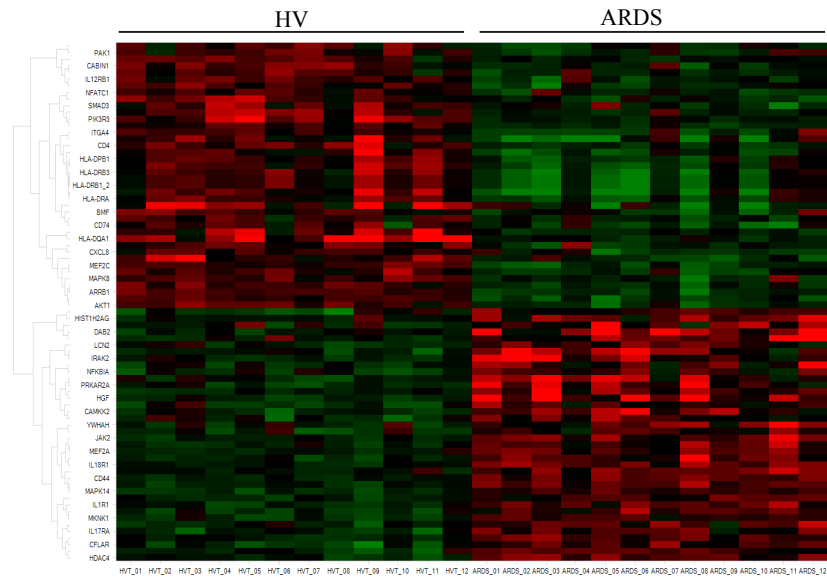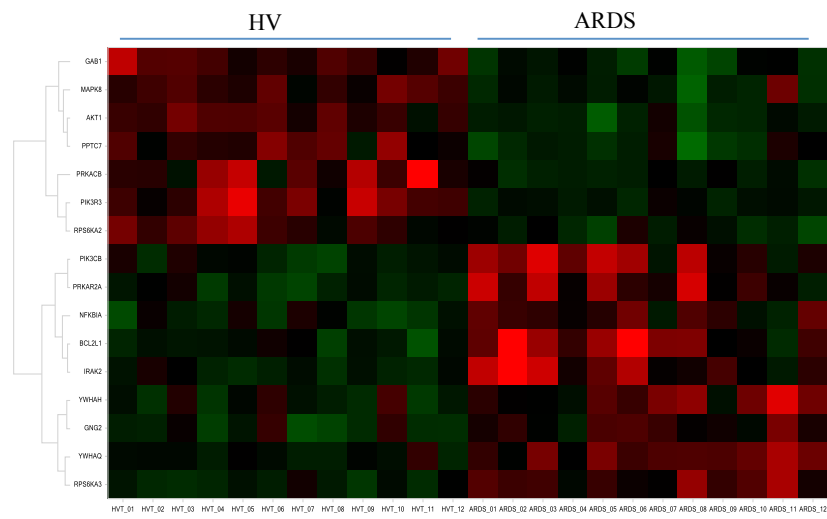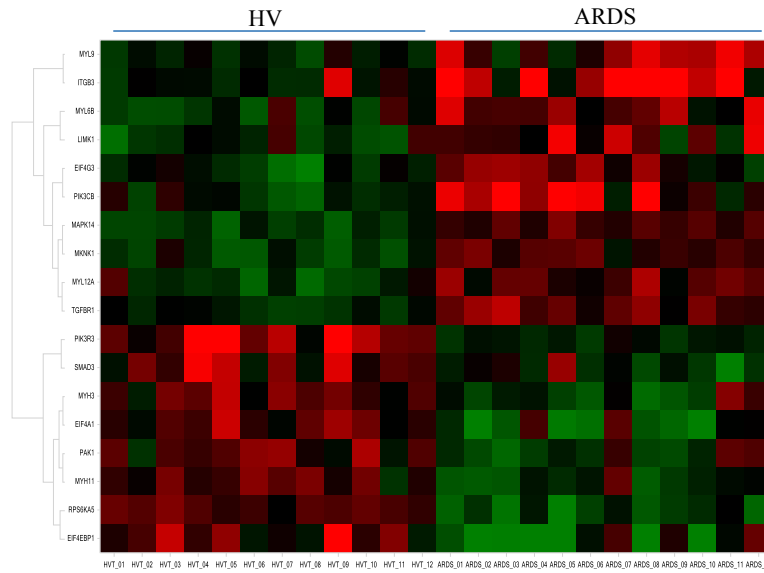
A. Immune response

B. Apoptosis

C. Cytoskeletal remodelling

D. Mucin production

42 Juss et al. 2015

Juss et al. 2015
Supplementary Figure S4